© creative

Scientific paper

## Preparation, Structures, Photoluminescence and Semiconductive Properties of Two New Lanthanide Mercury Materials with a 3-D Framework Structure

Hao-Dong Liu,<sup>1</sup> Xi-Yu Shao,<sup>1</sup> Yu-Yue Xu,<sup>1</sup> Wen-Tong Chen,\*,<sup>1,2</sup> Cheng Liu,\*,<sup>1</sup> Sheng-Ping Dai<sup>1</sup> and Chang-Wang Pan<sup>1</sup>

<sup>1</sup> Institute of Applied Chemistry, School of Chemistry and Chemical Engineering, Ji'an Key Laboratory of Photoelectric Crystal Materials and Device, Humic Acid Utilization Engineering Research Center of Jiangxi Province, Jiangxi Province Key Laboratory of Coordination Chemistry, Jinggangshan University, 343009, Ji'an, Jiangxi, China

<sup>2</sup> Department of Ecological and Resources Engineering, Fujian Key Laboratory of Eco-Industrial Green Technology, Wuyi University, 354300, Wuyishan, Fujian, China

> \* Corresponding author: E-mail: wtchen\_2000@aliyun.com (W.-T. Chen); 234871279@qq.com (C. Liu) +86(796)8100490; fax +86(796)8100490

> > Received: 02-05-2024

#### **Abstract**

Two new lanthanide mercury materials,  $[Gd(IA)_3(H_3O)_2Hg_3Br_6]_nCl_{2n}$  (1) and  $[La(IA)_3(H_3O)_2Hg_3Br_6]_nCl_{2n}$  (2) (IA = isonicotinic anion), have been prepared under solvothermal conditions and characterized by single-crystal X-ray diffraction techniques. They are isomorphic and characterized by a three-dimensional (3-D) framework structure. The lanthanide ions are bound by eight oxygen atoms to exhibit a square antiprismatic geometry. The solid-state photoluminescence experiment discovers that compound 1 shows a strong emission in the red region. Compound 1 possesses CIE (Commission Internationale de l'Éclairage) chromaticity coordinates of 0.7347 and 0.2653. Its CCT (correlated color temperature) is 6514 K. Compound 2 displays yellow photoluminescence and it has CIE chromaticity coordinates of 0.4411 and 0.5151. The CCT of compound 2 is 3633 K. Solid-state UV/Vis diffuse reflectance spectra revealed that their semiconductor band gaps are 2.16 eV and 2.85 eV, respectively.

Keywords: Lanthanide; mercury; photoluminescence; band gap; semiconductor

#### 1. Introduction

For several decades, lanthanide coordination compounds have received more and more attention from chemical and material researchers, because lanthanide coordination compounds generally exhibit useful physicochemical properties such as photoluminiscence, catalyst, magnet and biochemical sensors, which makes them attractive in display, catalysis, medical and other applications fields.  $^{1-6}$  The interesting physicochemical properties of lanthanide coordination compounds dominantly rise from the rich 4f electron of the lanthanide ion. Among these attractive physicochemical properties, photoluminiscence is especially interesting. Lanthanide coordination compounds generally show strong photoluminescence emission if the 4f electron transition can efficiently occur.

People have so far completed a lot of exploration about lanthanide coordination compounds, in order to find out their potential use in the areas of electrochemical displays, luminescent sensors, medicine, magnetic material, light-emitting diode, and so on.<sup>7–12</sup>

Zinc, cadmium and mercury are group 12 (IIB) elements and they have also attracted a lot of attention because of the following reasons: vital roles played by zinc in biological systems, various coordination motifs, attractive photoelectric and photoluminescence behavior, and so forth. Moreove, the IIB elements can also be applied for synthesizing semiconductor materials and, to this day, many semiconductor materials containing IIB elements have been documented. 17–20

Organic molecules with different functional groups are very useful in the construction of metal coordination

compounds. N-containing heterocyclic molecules (for instance, isonicotic acid, nicotic acid, 4,4'-bipy, 2,2'-bipy, etc.) have been widely applied for the preparation of metal coordination compounds because of their rich coordination sites and various coordination modes.<sup>21-23</sup> To our knowledge, isonicotinic acid is an useful building molecule because it possesses two carboxylic oxygen atoms at one side and one nitrogen atom at the other side. As a result, isonicotinic acid molecules can bind to different metal ions to form new compounds. Isonicotic acid molecules are deemed to be a nice chelating and bridging ligand to form metal coordination compounds with high dimensional extended structures. Furthermore, the pyridyl ring of isonicotic acid molecule possesses delocalized  $\pi$ -electrons which endow isonicotic acid molecules to be a good candidate to prepare luminescent materials in the fields of organic light emitting diode (OLED), chemical sensor, solar energy conversion, and so forth.<sup>24–26</sup>

During these years, our group keeps exploring the photoluminescence, magnetism and semiconductor materials. We recently become interested in the crystal engineering of lanthanide IIB materials. For the sake of investigating new lanthanide IIB materials with new structural motifs and attractive performance, we focus on the design and preparation of new lanthanide IIB materials with various organic molecules by means of solvothermal reactions. In this research, we report the preparation, crystal structures, photoluminescence, CIE, CCT, FT-IR, PXRD (powder X-ray diffraction) and semiconductive investigation of two new lanthanide mercury compounds with a 3-D framework structure, namely, [Gd(IA)<sub>3</sub>(H<sub>3</sub>O)<sub>2</sub>Hg<sub>3</sub>  $Br_6]_nCl_{2n}$  (1) and  $[La(IA)_3(H_3O)_2Hg_3Br_6]_nCl_{2n}$  (2) (IA = isonicotinic anion) which were prepared through solvothermal reactions.

### 2. Experimental

#### 2. 1. Instruments and Chemicals

All of the chemicals used for the reactions were commercially bought and directly applied for the syntheses of the title compounds. The C, H and N elemental analyses were performed on an Elementar Vario EL elemental analyzer. The FT-IR spectroscopy were conducted on a PE Spectrum-One FT-IR spectrophotometer with a KBr pellet and the wavenumber is in the span of  $400 \text{ cm}^{-1} \sim 4000 \text{ cm}^{-1}$ . The PXRD pattern was obtained on a AL-Y3000 powder diffractometer with Cu-K ( $\lambda = 1.54056 \text{ Å}$ ),  $10^{\circ} \le 2\theta \le 50^{\circ}$ , 0.1° step size, and one second of exposure time. The theoretical powder curve was obtained from the X-ray single-crystal diffraction data set and processed using the free version of Mercury v1.4 program software offered by the Cambridge Crystallographic Data Centre. The photoluminescence spectra were carried out on a F97XP photoluminescence spectrometer with the wavelength in the range of 200 nm ~ 900 nm. The solid-state UV/Vis diffuse reflectance spectra

were measured on a TU1901 UV /Vis spectrometer with the wavelength in the range of 190 nm  $\sim$  900 nm.

#### 2. 2. Synthesis of $[Gd(IA)_3(H_3O)_2Hg_3Br_6]_nCl_{2n}$ (1)

The Gd(NO<sub>3</sub>)<sub>3</sub>·6H<sub>2</sub>O (0.5 mmol, 452 mg; Sigma-Aldrich company, analytical reagent, CAS # 19598-90-4), HgBr<sub>2</sub>(1.5 mmol, 540 mg; Sigma-Aldrich company, analytical reagent, CAS # 7789-47-1), isonicotinic acid (1.5 mmol, 185 mg; Sigma-Aldrich company, analytical reagent, CAS # 55-22-1), concentrated hydrochloric acid (0.1 mL; Sigma-Aldrich company, analytical reagent, CAS # 7647-01-0) and distilled water (10 mL) were mixed into a 25 mL Teflon-lined stainless steel autoclave. The autoclave was heated at 433 K for ten days and powered off. After naturally cooling down to room temperature, yellow crystals suitable for the single-crystal X-ray diffraction measurement were collected, washed with distilled water and dried in air. The yield was 41% (based on  $Gd(NO_3)_3 \cdot 6H_2O$ ).  $C_{18}H_{18}Br_6Cl_2Gd$ Hg<sub>3</sub>N<sub>3</sub>O<sub>8</sub>: calc. C, 12.62; H, 1.06; N, 2.45; Found C,

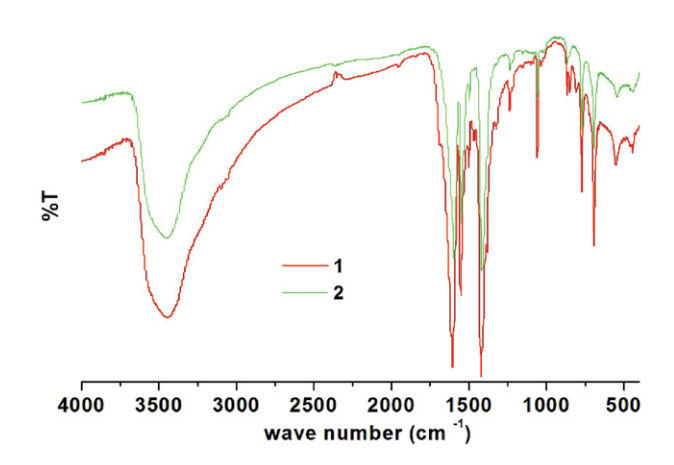


Fig. 1: FT-IR spectroscopy of 1 and 2.

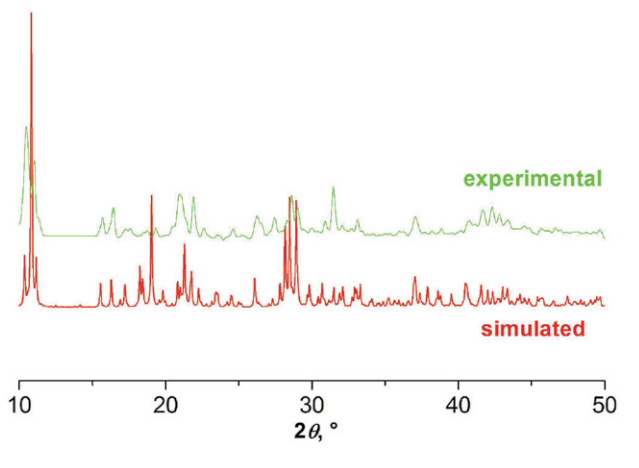


Fig. 2: PXRD of 1.

12.69; H, 1.09; N, 2.51. FT-IR peaks (KBr, cm<sup>-1</sup>): 3440(vs), 1950(w), 1607(vs), 1551(s), 1500(w), 1420(vs), 1233(m), 1062(s), 864(w), 809(w), 768(s), 693(s), 552(m) and 440(w), as shown in Fig. 1. The purity is confirmed by PXRD, as shown in Fig. 2.

# 2. 3. Synthesis of [La(IA)<sub>3</sub>(H<sub>3</sub>O)<sub>2</sub>Hg<sub>3</sub>Br<sub>6</sub>]<sub>n</sub>Cl<sub>2n</sub> (2)

The La(NO<sub>3</sub>)<sub>3</sub>·6H<sub>2</sub>O (0.5 mmol, 217 mg; Sigma-Aldrich company, analytical reagent, CAS # 10277-43-7), HgBr<sub>2</sub>(1.5 mmol, 540 mg; Sigma-Aldrich company, analytical reagent, CAS # 7789-47-1), isonicotinic acid (1.5 mmol, 185 mg; Sigma-Aldrich company, analytical reagent, CAS # 55-22-1), concentrated hydrochloric acid (0.1 mL; Sigma-Aldrich company, analytical reagent, CAS # 7647-01-0) and distilled water (10 mL) were mixed into a 25 mL Teflon-lined stainless steel autoclave. The autoclave was heated at 433 K for ten days and powered off. After naturally cooling down to room temperature, colorless crystals suitable for the single-crystal X-ray diffraction measurement were collected, washed with distilled water and dried in air. The yield was 34% (based on La(NO<sub>3</sub>)<sub>3</sub>·6H<sub>2</sub>O).  $C_{18}H_{18}Br_6Cl$ <sub>2</sub>Hg<sub>3</sub>LaN<sub>3</sub>O<sub>8</sub>: calc. C, 12.75; H, 1.07; N, 2.48; Found C, 12.80; H, 1.11; N, 2.52. FT-IR peaks (KBr, cm<sup>-1</sup>): 3444(vs), 1950(w), 1596(vs), 1551(s), 1501(w), 1415(vs), 1234(m), 1056(s), 865(w), 769(s), 688(s), 547(m) and 438(w), as shown in Fig. 1. The purity is confirmed by PXRD, as shown in Fig. 3.

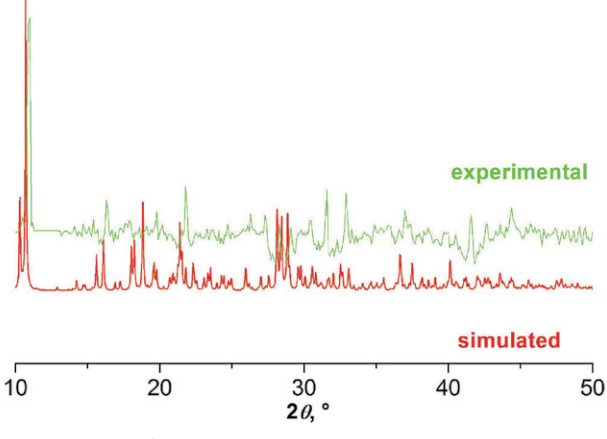


Fig. 3: PXRD of 2.

#### 2. 4. X-ray structure determination

The crystal data sets of the title compounds were measured using a Rigaku Mercury CCD X-ray diffractometer equipped with graphite monochromated Mo-K $\alpha$  radiation source with a wavelength being of 0.71073 Å. The measurements were conducted with the use of an  $\omega$  scan mode. The data reduction and empirical absorption corrections were performed by using the CrystalClear software. The crystal structures were solved by means of the direct methods. The Siemens SHELXTLTM Version 5 software packages were used to solve the structures. All of the non-hydrogen atoms were found based on the subsequent difference electron density maps and refined anisotropi-

Table 1: Crystallographic data and structural analyses for the title compounds

Compound	1	2
Formula	C <sub>18</sub> H <sub>18</sub> Br <sub>6</sub> Cl <sub>2</sub> GdHg <sub>3</sub> N <sub>3</sub> O <sub>8</sub>	C <sub>18</sub> H <sub>18</sub> Br <sub>6</sub> Cl <sub>2</sub> Hg <sub>3</sub> LaN <sub>3</sub> O <sub>8</sub>
$M_r$	1713.73	1695.39
Color	yellow	colorless
Crystal size/mm	0.14 0.11 0.09	0.19 0.04 0.03
Crystal system	Monoclinic	Monoclinic
Space group	$P2_1/n$	$P2_1/n$
a (Å)	12.5309(6)	12.4632(4)
b (Å)	9.7214(3)	9.8237(3)
c (Å)	32.7114(8)	33.0857(8)
β (°)	94.253(3)	94.448(3)
$V(Å^3)$	3973.9(2)	4038.6(2)
Z	4	4
$2 heta_{ m max}$ /°	50	50
Reflections collected	16417	21697
Independent, observed reflections ( $R_{int}$ )	5307, 4087 (0.0569)	6926, 5180 (0.0435)
$d_{\rm calcd.}$ (g/cm <sup>3</sup> )	2.864	2.788
$\mu/\mathrm{mm}^{-1}$	19.406	18.510
T/K	293(2)	293(2)
F(000)	3036	3008
$R_1$ , $wR_2$	0.0787, 0.1746	0.0629, 0.1447
S	1.027	1.072
Largest and mean $\Delta/\sigma$	0.002, 0.000	0.002, 0.000
$\Delta \rho$ (max, min) (e/Å <sup>3</sup> )	1.731, -1.407	2.574, -1.785

cally, while all hydrogen atoms were theoretically located. The final structures were refined by using the full-matrix least-squares refinement on  $F^2$ . Crystallographic data and structural analyses for the title compounds are listed in Table 1. Selected bond lengths and bond angles are presented in Table S1.

#### 3. Result and Discussions

The FT-IR spectroscopy of the title compounds were conducted at room temperature. The FT-IR peaks of the title compounds are mainly found in the frequency range of 500 cm<sup>-1</sup>  $\sim$  1600 cm<sup>-1</sup>, as shown in Fig. 1. The FT-IR spectroscopy of the title compounds are very similar, because they are isomorphic. The very strong intensity peaks at 3440 cm<sup>-1</sup> and 3444 cm<sup>-1</sup> can be assigned to the O-H asymmetric vibration of the water molecules. The very strong peaks at 1607 cm<sup>-1</sup> and 1596 cm<sup>-1</sup> should be ascribed to the stretching vibrations of the C=O bonds. The peaks at 1551 cm<sup>-1</sup>, 1420 cm<sup>-1</sup>, 1415 cm<sup>-1</sup>, 1233 cm<sup>-1</sup> and 1234 cm<sup>-1</sup> can be ascribed to the stretching vibrations of the pyridyl ring of the isonicotinic ligands. The peaks locating in the range of 864 cm<sup>-1</sup> ~ 1062 cm<sup>-1</sup> can be assigned to the bending vibration of the pyridyl ring of the isonicotinic ligands. The peaks at 438 cm<sup>-1</sup> ~ 769 cm<sup>-1</sup> can be ascribed to the stretching vibrations of the Hg-Br bonds.

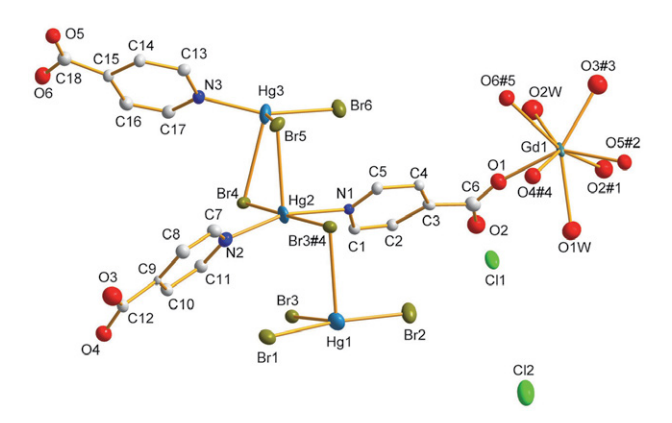


**Fig. 4:** An ORTEP figure of **1** with 25% thermal ellipsoids. Hydrogen atoms were omitted for clarity.

As discovered by the single-crystal X-ray diffraction measurements, compounds 1 and 2 are isomorphic. They crystallize in the space group  $P2_1/n$  of the monoclinic system with four formula units in one cell. In this section only the crystal structure of compound 1 is described herein as an example. The crystallographically asymmetric unit is comprised of one  $Gd^{3+}$  cation, three  $Hg^{2+}$  cations, six  $Br^-$  anions, two isolated  $Cl^-$  anions, three isonicotinic acid anions and two water molecules, as presented in Fig. 4. All of the crystallographic independent atoms are resided at general positions. The  $Gd^{3+}$  cation is coordinated by eight oxy-

gen atoms, of which two come from two coordination water molecules and six are offered by six isonicotinic acid ligands, to yield a square antiprismatic GdO<sub>8</sub> motif. All water molecules are bound to the Gd<sup>3+</sup> cation. The Gd–O bond length locates in the span of 2.304(7) Å ~ 2.538(9) Å with an average value of 2.392(10) Å, as listed in Table S1. The Gd–O bond lengths are in the normal range and comparable with the values documented in the references. <sup>27,28</sup> The O–Gd–O bond angle is in the span of 69.2(3)° ~ 144.2(3)°. All of the isonicotinic acid molecule act as a  $\mu_3$ -bridging ligand with two oxygen atoms coordinating to two Gd<sup>3+</sup> cations and one nitrogen atom binding to one Hg<sup>2+</sup> cation (Fig. 4). The Gd<sup>3+</sup> cations are linked by two or four isonicotinic acid ligands to form a one-dimensional (1-D) [Gd(IA)<sub>3</sub>(H<sub>3</sub>O)<sub>2</sub>]<sub>n</sub> chain running along the *b* axis, as presented in Fig. 5.

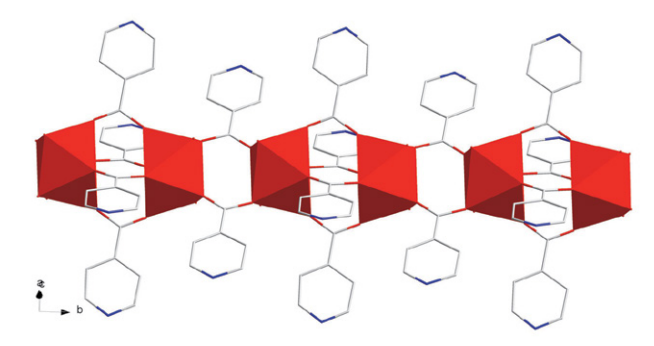


**Fig. 5:** A 1-D  $[Gd(IA)_3(H_3O)_2]_n$  chain of **1** in polyhedral and wires representation. The polyhedron is  $GdO_8$ .

The three mercury ions are grouped into three types. The Hg1 is surrounded by four Br<sup>-</sup> anions to give a distorted HgBr<sub>4</sub> tetrahedron. The Hg3 is coordinated by three Br<sup>-</sup> anions and one nitrogen atom to form a distorted HgBr<sub>3</sub>N tetrahedron. Differently, the Hg2 is coordinated by three Br<sup>-</sup> anions and two nitrogen atoms to yield a distorted Hg-Br<sub>3</sub>N<sub>2</sub> pyramid. The bond lengths of Hg-Br are in the range of 2.4128(11) Å ~ 3.1143(10) Å with an average value of 2.8202(12) Å, as listed in Table S1. The Hg-Br bond lengths are in the normal range and comparable with the values documented in the references. 29,30 The Br-Hg-Br bond angle is in the span of 89.23(3)° ~ 175.15(3)°. The Hg-Br-Hg bond angles are in the range of 82.11(3)° ~ 178.45(3)°. The bond lengths of Hg-N are in the span of  $2.136(7) \text{ Å} \sim 2.230(6) \text{ Å}$  with an average value of 2.171(8)Å. The Hg-N bond lengths are in the normal range and comparable with the values documented in the references. 31,32 The N-Hg-Br bond angle is in the span of  $85.89(16)^{\circ} \sim 156.81(19)^{\circ}$ . The N(2)-Hg(2)-N(1) bond angle is 162.7(3)° which is almost linear, as shown in Fig. 4. The mercury ions are connected by the Br<sup>-</sup> anions to yield a 1-D  $[Hg_3Br_6]_n$  chain running along the b direction, as presented in Fig. 6. The 1-D [Hg<sub>3</sub>Br<sub>6</sub>]<sub>n</sub> chains and the above mentioned 1-D  $[Gd(IA)_3(H_3O)_2]_n$  chains are interlinked by the isonicotinic acid ligands to yield a two-dimensional (2-D) layer extending along the bc plane, as

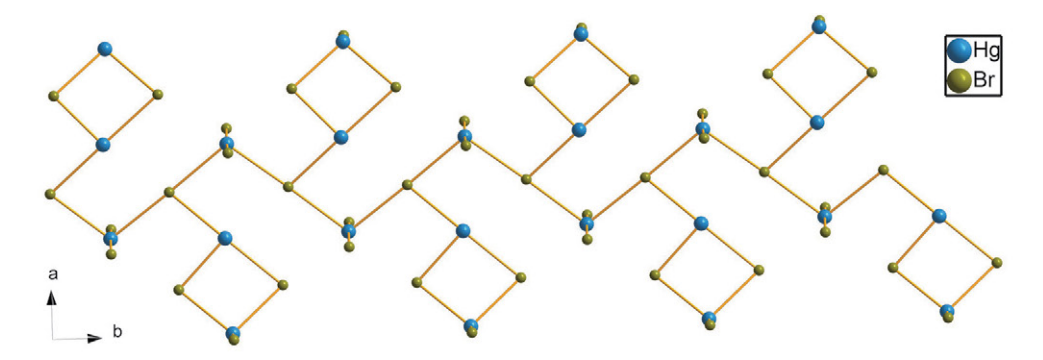


**Fig. 6:** A 1-D  $[Hg_3Br_6]_n$  chain in **1**.

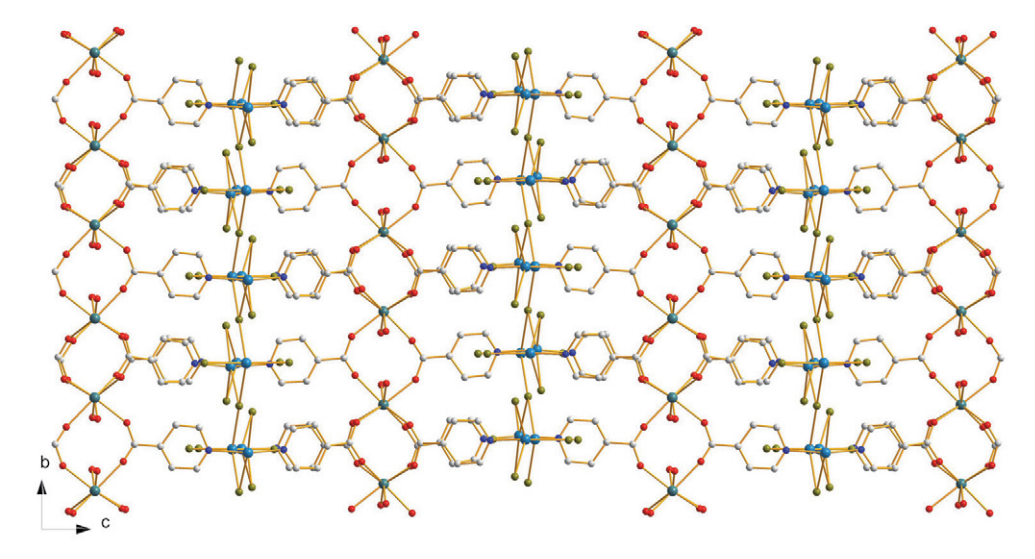


Fig. 7: A 2-D layer in 1.

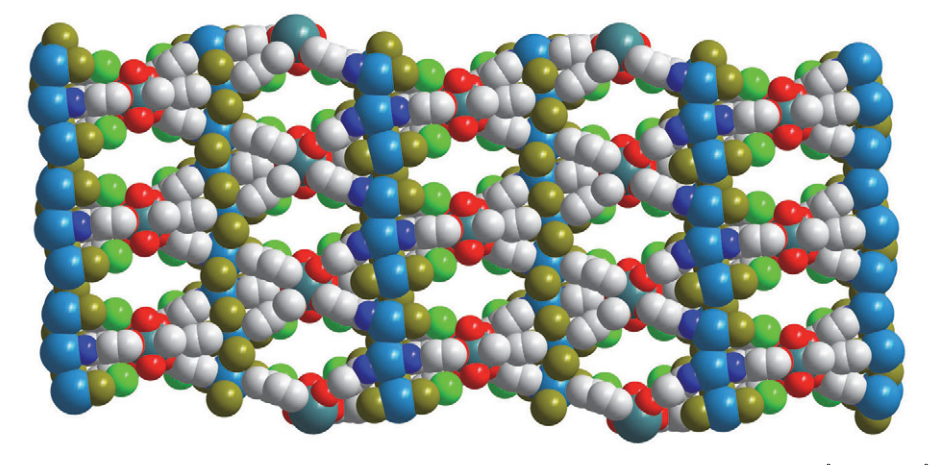


Fig. 8: The 3-D framework structure of 1 in space-filling representation with the channel window size being of 8.057  $\text{Å} \times 14.879 \ \text{Å}$ .

displayed in Fig. 7. The 2-D layers are further interconnected together to construct a three-dimensional (3-D) framework structure with the channel window size being of  $8.057~\text{Å} \times 14.879~\text{Å}$ , as shown in Fig. 8.

It is well-known that many lanthanide coordination compounds can exhibit photoluminescence emissions. Therefore, both of the title compounds are possible to display photoluminescence performance because they have lanthanide ions. Based on such a thought, the powder samples of compounds 1 and 2 were adopted to carry out their photoluminescence measurements under room temperature. The results of the photoluminescence measurements are shown in Fig. 9 and Fig. 11. With regard to compound 1, when it was excited by the 284 nm light, it

displayed red photoluminescence with an emission band locating at 740 nm, as presented in Fig. 9. Compound 1 possesses CIE (Commission Internationale de l'Éclairage) chromaticity coordinates of 0.7347 and 0.2653, as shown in Fig. 10. Its CCT (correlated color temperature) is 6514 K. As a result, compound 1 is expected to be a potential red light photoluminescent material. As for compound 2, when it was excited by the 322 nm UV light, it shows yellow photoluminescence with the emission band locating at 561 nm, as presented in Fig. 11. Compound 2 possesses remarkable CIE chromaticity coordinates of 0.4411 and 0.5151, as displayed in Fig. 12. The CCT for compound 2 is 3633 K. As a result, compound 2 is expected to be a potential yellow light photoluminescent material. The photoluminescence features of compounds 1 and 2 are clearly dif-

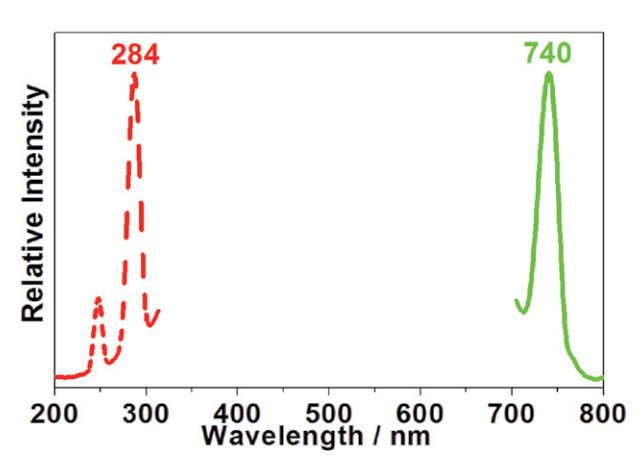


Fig. 9: Solid state photoluminescence spectra of 1 with the red and green lines representing excitation and emission spectra, respectiely.

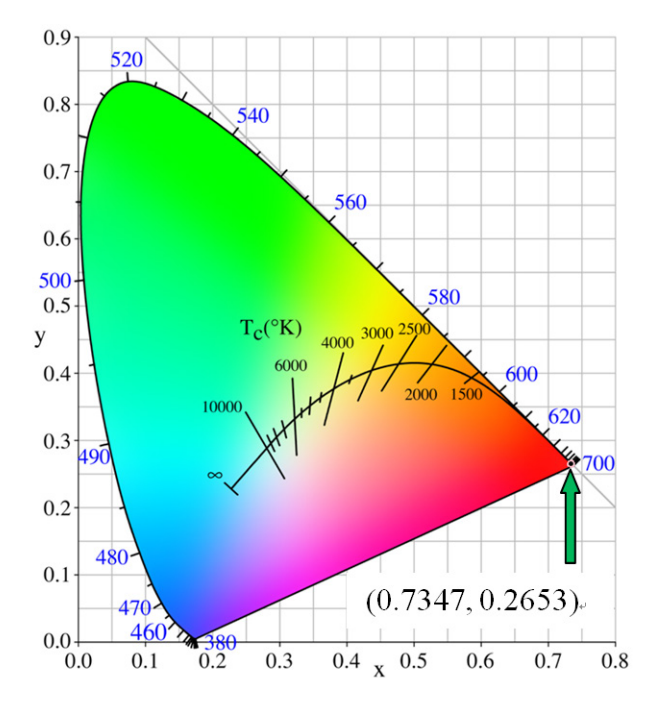


Fig. 10: CIE diagram of 1.

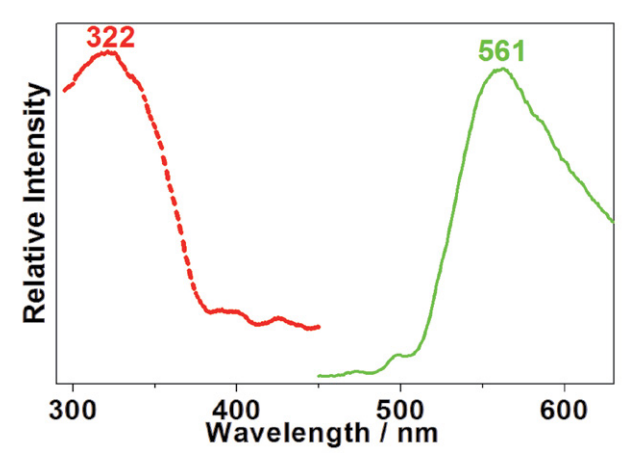


Fig. 11: Solid state photoluminescence spectra of 2 with the red and green lines representing excitation and emission spectra, respectively.

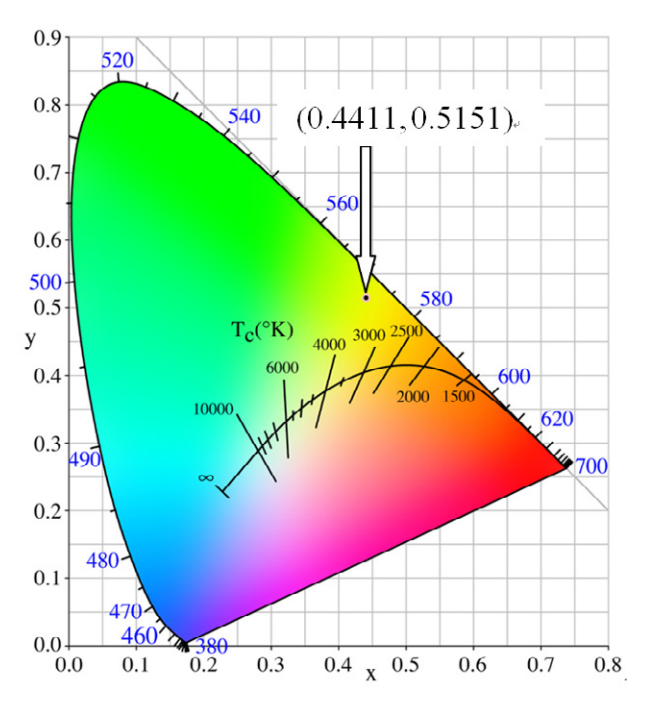


Fig. 12: CIE diagram of 2.

ferent, although they have isomorphic crystal structures. This suggests that the lanthanide ions plays important role for their photoluminescence performances.

The photoluminescence performances, catalytic properties and magnetic behavior of lanthanide coordination compounds have thus far been broadly investigated, however, their semiconductor performances have been rarely studied. Because of such a reason and in order to more deeply investigate the physicochemical properties of both title compounds, the solid state UV/Vis diffuse reflection experiments were conducted with finely ground powder samples under room termperature. The solid state UV/Vis diffuse reflectance spectrum data sets for both title compounds were processed by means of the well-known

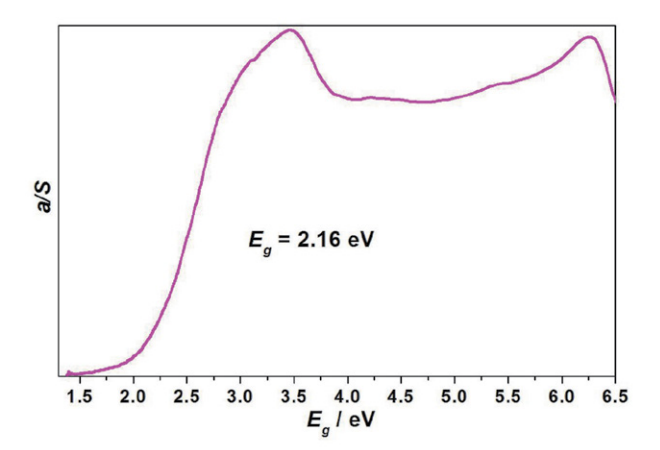


Fig 13: The UV-vis diffuse reflectance curve measured with solid state samples of 1.

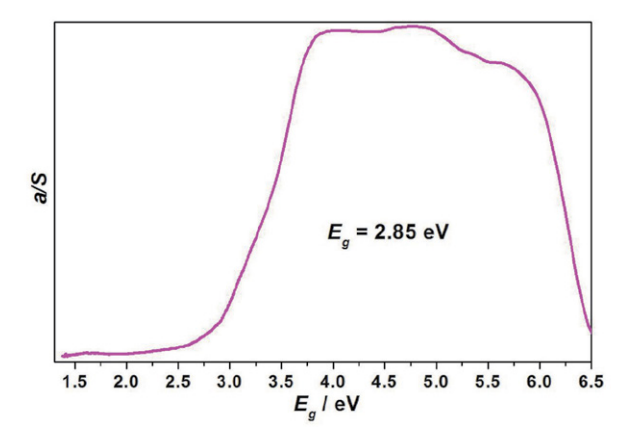


Fig 14: The UV-vis diffuse reflectance curve measured with solid state samples of 2.

Kubelka-Munk formula  $\alpha/S = (1-R)^2/2R$ , of which the  $\alpha$  is the absorption coefficient, S means the scattering coefficient, while R refers to the reflection coefficient. The transferred solid state UV/Vis diffuse reflectance spectra are shown in Fig. 13 and Fig. 14 for compounds 1 and 2, respectively. The semiconductor band gap for both title compounds were determined by means of the straight line epitaxy method from the maximum absorption edge of the  $\alpha/S$  versus energy curve. Based on such a method, the semiconductor band gaps for compounds 1 and 2 can be determined as 2.16 eV and 2.85 eV, respectively. Moreover, the solid state UV/Vis diffuse reflectance diagrams of both title compounds discover that their absorption edges are not steep. This suggests that both title compounds have gone through an indirect transition process.<sup>33</sup> Therefore, the title compounds are probably candidates for wide band gap semiconductive materials.

#### 4. Conclusions

In conclusion, we have prepared two new lanthanide mercury materials via a solvothermal reaction. They are

isomorphic and characterized by a 3-D framework structure. They exhibit red or yellow photoluminescent emissions with different CIE and CCT values. This suggests that they are a potential red or yellow light photoluminescent material in display and other imaging fields. The solid state UV/Vis diffuse reflectance spectrum reveals that they are probably candidates for wide band gap semiconductive materials. Both of the photoluminescence features and semiconductor performances for compounds 1 and 2 are obviously different, although they show isomorphic crystal structures and only metal ions are different. This indicates that the lanthanide ions play a very vital role for their photoluminescence features and semiconductor performances. Therefore, using other lanthanide ions, similar compounds with new properties may be obtained. More explorations on the relationship between the crystal structure and the physicochemical performance in this field are in progress in our group.

#### Acknowledgements

This work was supported by the National Natural Science of Foundation of China (22265014), the Science and Technology Project of Jiangxi Provincial Department of Education (GJJ2201602), and the Science and Technology Planning Project of Nan Ping, Fujian, China (N2020Z008).

#### Supplementary Material

Crystallographic data for the structure reported in this paper have been deposited with the Cambridge Crystallographic Data Centre as supplementary publication no. CCDC 2330402 and 2330403 for compounds 1 and 2, respectively. Copies of the data can be obtained free of charge on application to CCDC, 12 Union Road, Cambridge CB2 1EZ, UK (fax: (44) 1223 336-033; e-mail: deposit@ccdc. cam.ac.uk

#### 7. References

- P. Ivanchenko, G. Escolano-Casado, L. Mino, L. Dassi, J. F. Fernandez-Sánchez, G. Martra, J. Gómez-Morales, Colloid. Surface. B 2022, 217, 112620.
  - **DOI:**10.1016/j.colsurfb.2022.112620
- Z. Z. Z. Weng, C. L. Chen, L. W. Ye, L. S. Long, L. S. Zheng, X. J. Kong, Sci. China Chem. 2023, 66, 443–448.
   DOI:10.1007/s11426-022-1493-y
- W. M. Wang, N. Qiao, J. L. Wang, Y. Chen, J. C. Yan, C. Y. Xu, C. S. Cao, *Catal. Today* 2024, 425, 114359.
   DOI:10.1016/j.cattod.2023.114359
- Q. Fan, C. Sun, B. L. Hu, Q. Wang, Mater. Today Bio. 2023, 20, 100646. DOI:10.1016/j.mtbio.2023.100646
- H. Jia, N. Li, H. Y. He, X. C. Zhang, Y. Y. Teng, W. P. Qin, Adv. Opt. Mater. 2024, DOI10.1002/adom.202302583.

- F. Pointillart, K. Bernot, B. Le Guennic, O. Cador, Chem. Commun. 2023, 59, 8520–8531. DOI:10.1039/D3CC01722B
- X. T. Dong, M. Q. Yu, Y. B. Peng, G. X. Zhou, G. Peng, X. M. Ren, *Dalton Trans.* 2023, 52, 12686–12694.
   DOI:10.1039/D3DT02106H
- J. R. Thomas, M. J. Giansiracusa, R. A. Mole, S. A. Sulway, Cryst. Growth Des. 2023, 24, 573–583.
   DOI:10.1021/acs.cgd.3c01380
- K. Nehra, A. Dalal, A. Hooda, P. Kumar, D. Singh, S. Kumar,
   R. S. Malik, P. Kumar, J. Lumin. 2023, 249.
   DOI:10.1016/j.jlumin.2022.119032
- A. Dalal, K. Nehra, A. Hooda, D. Singh, P. Kumar, S. Kumar,
   R. S. Malik, B. Rathi, *Inorg. Chim. Acta* 2023, 550, 121406.
   DOI:10.1016/j.ica.2023.121406
- Y. J. Chen, C. X. Dou, P. P. Yin, J. T. Chen, X. G. Yang, B. Li, L. F. Ma, L. Y. Wang, *Dalton Trans.* 2023, 52, 13872–13877.
   DOI:10.1039/D3DT01869E
- 12. K. M. Zhu, H. Y. Xu, Z. Y. Wang, Z. L. Fu, *Inorg. Chem. Front.* **2023**, *10*, 3383–3395. **DOI:**10.1039/D3QI00529A
- M. Arici, Cryst. Growth Des. 2017, 17, 5499–5505.
   DOI:10.1021/acs.cgd.7b01024
- B. Mohapatra, S. Verma, Cryst. Growth Des. 2013, 13, 2716– 2721. DOI:10.1021/cg4006168
- L. N. Wang, L. Fu, J. W. Zhu, Y. Xu, M. Zhang, Q. You, P. Wang, J. Qin, *Acta Chim. Slov.* 2017, 64, 202–207.
   DOI:10.17344/acsi.2016.3109
- P. Wang, Y. S. Wu, X. M. Han, S. S. Zhao, J. Qin, Acta Chim. Slov. 2017, 64, 431–437. DOI:10.17344/acsi.2017.3268
- Y. Yoshida, H. Ito, Y. Nakamura, M. Ishikawa, A. Otsuka, H. Hayama, M. Maesato, H. Yamochi, H. Kishida, G. Saito, Cryst. Growth Des. 2016, 16, 6613–6630.
   DOI:10.1021/acs.cgd.6b01294
- 18. L. Zhang, H. Lin, Y. Wu, S. Zhuo, *Chem. Phys. Lett.* **2016**, *661*, 224–227. **DOI:**10.1016/j.cplett.2016.08.079
- Y. Zeng, D. F. Kelley, J. Phys. Chem. C 2016, 120, 17853– 17862. DOI:10.1021/acs.jpcc.6b06282
- 20. T. Uematsu, E. Shimomura, T. Torimoto, S. Kuwabata, *J. Phys. Chem. C* **2016**, *120*, 16012–16023.

- **DOI:**10.1021/acs.jpcc.5b12698
- E. E. Moushi, A. Kourtellaris, I. Spanopoulos, M. J. Manos,
   G. S. Papaefstathiou, P. N. Trikalitis, A. J. Tasiopoulos, *Cryst. Growth Des.* 2015, 15, 185–193. DOI:10.1021/cg501141m
- L. B. Zhu, F. Li, M. L. Sun, Y. Y. Qin, Y. G. Yao, Chinese J. Struct. Chem. 2021, 40, 1031–1038.
- Y. L. Liu, Y. X. Zhao, J. H. Zhang, Y. Ye, Q. Q. Sun, J. Solid State Chem. 2022, 313, 123332. DOI:10.1016/j.jssc.2022.123332
- F. E. Özbek, M. Sertçelik, M. Yüksek, G. Ugurlu, A. M. Tonbul, H. Necefoglu, T. Hökelek, *J. Fluoresc.* 2019, 29, 1265–1275.
   DOI:10.1007/s10895-019-02440-x
- J. F. Zhang, J. J. Wu, G. D. Tang, J. Y. Feng, F. M. Luo, B. Xu, C. Zhang, Sensor Actuat. B-Chem. 2018, 272, 166–174.
   DOI:10.1016/j.snb.2018.05.121
- N. N. Pang, D. X. Lin, Z. Y. Zhan, X. D. Ding, T. T. Shi, Q. X. Meng, P. Y. Liu, W. G. Xie, *Mat. Sci. Semicon. Proc.* 2022, 145, 106639. DOI:10.1016/j.mssp.2022.106639
- A. Hernandez, J. Jenkins, H. Maslen, M. Zeller, G. Horner, C. Dempsey, J. Urteaga, C. Dunlap, R. A. Zehnder, *Inorg. Chim. Acta* 2018, 471, 104–112. DOI:10.1016/j.ica.2017.10.001
- 28. T. Jiang, J. Zhou, R. Li, H.-H. Zou, L. Fu, *Inorg. Chim. Acta* **2018**, *471*, 377–383. **DOI:**10.1016/j.ica.2017.11.032
- 29. L. K. Rana, S. Sharma, G. Hundal, *J. Mol. Struct.* **2018**, *1153*, 324–332. **DOI:**10.1016/j.molstruc.2017.10.015
- S. J. Sabounchei, M. Ahmadianpoor, A. Hashemi, F. Mohsenzadeh, R. W. Gable, *Inorg. Chim. Acta* 2017, 458, 77–83.
   DOI:10.1016/j.ica.2016.12.023
- V. Amani, R. Alizadeh, H. S. Alavije, S. F. Heydari, M. Abafat, *J. Mol. Struct.* 2017, 1142, 92–101.
   DOI:10.1016/j.molstruc.2017.04.034
- M. Khanpour, A. Naghipour, A. A. Tehrani, A. Morsali, D. Morales-Morales, S. Hernandez-Ortega, J. Mol. Struct. 2017, 1135, 26–31. DOI:10.1016/j.molstruc.2017.01.024
- S. F. M. Schmidt, C. Koo, V. Mereacre, J. Park, D. W. Heermann, V. Kataev, C. E. Anson, D. Prodius, G. Novitchi, R. Klingeler, A. K. Powell, *Inorg. Chem.* 2017, 56, 4796–4806.
   DOI:10.1021/acs.inorgchem.6b02682

#### Povzetek

Pod solvotermalnimi pogoji smo sintetizirali dve novi koordinacijski spojini živega srebra z lantanoidi,  $[Gd(IA)_3(H_3O)_2Hg_3Br_6]_nCl_{2n}$  (1) in  $[La(IA)_3(H_3O)_2Hg_3Br_6]_nCl_{2n}$  (2) (IA = izonikotinatni anion). Produkta smo karakterizirali z monokristalno rentgensko analizo. Spojini sta izomorfni in tvorita tridimenzionalno (3-D) ogrodje. Lantanoidni ioni so osemštevno koordinirani s kisikovimi atomi v obliki kvadratne antiprizme. Fotoluminiscenčne meritve v trdnem stanju kažejo, da ima spojina 1 močno emisijo v rdečem območju. Spojina 1 ima barvne koordinate CIE (Commission Internationale de l'Éclairage) 0.7347 in 0.2653. Njena vrednost korelirane barvne temperature (CCT) je 6514 K. Spojina 2 kaže rumeno fotoluminiscenco ter barvne koordinate CIE 0.4411 in 0.5151. Vrednost CCT za spojino 2 znaša 3633 K. Z meritvami UV/Vis v trdnem stanju smo določili širini prepovedanega pasu za obe spojini, ki znašata 2.16 eV in 2.85 eV.



Except when otherwise noted, articles in this journal are published under the terms and conditions of the Creative Commons Attribution 4.0 International License